

Synthesis and Characterization of $Ba_xMg_yAl_2O_4$: Eu, Dy nanophosphors Prepared Using Solution - Combustion Method

M. A. Kebede^{1,2} and F.B. Dejene^{1*}

¹Department of Physics, University of the Free State (Qwaqwa Campus), Private Bag X13, Phuthaditjhaba, 9866, South Africa

²Energy and Processes, Materials Science and Manufacturing, Council for Scientific and Industrial Research, P.O.Box 395, Pretoria, 0001, South Africa

E-mail: dejenebf@ufs.ac.za

Abstract. Europium-doped barium magnesium aluminate ($Ba_xMg_yAl_2O_4$:Eu) phosphors were obtained at low temperature using the solution - combustion of corresponding metal nitrate-urea solution mixtures. The particle sizes, morphology, structural and luminescent properties of the as-synthesized phosphors were examined by means of scanning electron microscopy (SEM), X-ray diffraction (XRD) and photoluminescence (PL). It was found that the change in Ba:Mg molar ratios showed great influence not only on the particle size and morphology, but also on their PL spectra and crystalline structure. The structure of $Ba_xMg_yAl_2O_4$ nanophosphors changes from a monoclinic structure for Ba 26 mole% to orthorhombic for Mg 26 mole% and a small change in peak position at high angles due to differences in size between Ba and Mg ions. The peak of the emission band occurs at longer wavelength (around 615nm) with increase in Mg concentration but display a broad band emission at 498 nm for lower Mg concentration. The blue-green emission is probably due to the influence of 5d electron states of Eu^{2+} in the crystal field because of atomic size variation causing crystal defects while the red emission is due to f-f transitions. This finding clearly demonstrate the possibility of fine tuning the colour emission and solid solubility limit in $Ba_xMg_yAl_2O_4$:Eu phosphors through the simple and a cheap process.

1. Introduction

Luminescent phosphors have gained abundant interest in their production for their potential applications in the development of different luminescent display systems [1–6]. Phosphors based on silicates, aluminates, germanate and other related oxides are of more interest nowadays. Aluminates generally generate more defect-related traps when they are doped with rare earth ions. Several aluminate compositions are investigated and used as photoluminescence (PL), catholuminescence and plasma display panel phosphors for their high quantum efficiency in the visible region. Eu^{2+} -doped phosphors usually show intense broad band PL with a short decay time of the order of tens of nanoseconds [7]. The emission of Eu^{2+} is strongly dependent on the host lattice and can occur from the ultraviolet to the red region of the electro-magnetic spectrum [8-9]. This is because the $5d \leftrightarrow 4f$ transition is associated with the change in electric dipole and the 5d excited state is affected by crystal

* To whom any correspondence should be addressed.

field effects. Notably barium and strontium aluminates have been reported to be good host material. Accordingly, the property of phosphor depends on their crystal structure of the mother phases.

Compared with sulfide phosphorescent phosphors, $\text{BaAl}_2\text{O}_4:\text{Eu,Dy}$ phosphor possesses safer, chemically stable, very bright and long-lasting photoluminescence with no radiation [10, 11]. The tuning of colors is controllable by the subtle structure modifications [12, 13]. For instance, the emissions of Eu^{2+} -doped MAl_2O_4 ($\text{M} = \text{Ba, Ca, Sr or Mg}$) are all in range of blue and green [14]. For long afterglow phosphors, it is well known that defect-related traps and trapping dynamics, which can be effectively adjusted by doping ions with various valences, play an important role in their luminescence and afterglow properties [14]. Also, controlling trap kinds and amount by co-doping ions is an efficient technique to study the long afterglow mechanism. In this paper, Mg^{2+} ion was used to study the co-doping effect on the luminescence and afterglow behavior of $\text{BaAl}_2\text{O}_4:\text{Eu,Dy}$ phosphor. The grain size of phosphor powders prepared through solid-state reaction method is in several tens of micrometers. Phosphors of small particles must be obtained by grinding the larger phosphor particles. Those processes easily introduce additional defects and greatly reduce luminescence efficiency [15]. With the development of scientific technologies on materials, several chemical synthesis techniques, such as co-precipitation [16], sol-gel [17] and combustion synthesis methods [18], have been applied to prepare nano-sized BaAl_2O_4 and/or its phosphors. Among the various wet chemical routes, the solution combustion technique has been regarded as one of the effective and economic methods due to its convenient processing, simple experimental setup and significant time-saving and high purity products [19-21]. In the present work, luminescence properties of Eu^{2+} doped $\text{BaAl}_2\text{O}_4\text{-MgAl}_2\text{O}_4$ ternary system prepared by a solution-combustion process is reported through emission, excitation, lifetime and structural from X-ray diffraction (XRD), SEM.

2. Experiments

$\text{Ba}_x\text{Mg}_y\text{Al}_2\text{O}_4:\text{Eu}^{2+}$ phosphor powders were prepared by a solutions combustion method without the use of flux material. $\text{Ba}(\text{NO}_3)_2$, $\text{Mg}(\text{NO}_3)_3 \cdot 9\text{H}_2\text{O}$, $\text{Al}(\text{NO}_3)_3 \cdot 9\text{H}_2\text{O}$, $\text{Eu}_2(\text{NO}_3)_3$ (4N) and $\text{CH}_4\text{N}_2\text{O}$ were used as starting materials. The procedure used to prepare $\text{Ba}_x\text{Mg}_y\text{Al}_2\text{O}_4:\text{Eu,Dy}$ had the following stages. Firstly, $\text{Al}(\text{NO}_3)_3 \cdot 9\text{H}_2\text{O}$, $\text{Mg}(\text{NO}_3)_3 \cdot 9\text{H}_2\text{O}$, $\text{Ba}(\text{NO}_3)_2$, $\text{Eu}_2(\text{NO}_3)_3$ and $\text{CO}(\text{NH}_2)_2$ were dissolved into deionised water and stirred at ambient temperature for $\frac{1}{2}$ hr to obtain transparent solution. After that, the precursor solution was introduced into a furnace preheated at 500°C and then white powders were obtained. To investigate the effect of the Ba/Mg molar ratios on the structural and PL properties of the $\text{Ba}_x\text{Mg}_y\text{Al}_2\text{O}_4:\text{Eu}^{2+}$ phosphor, samples with Ba/Mg molar ratios of 0 to 26 mol % were prepared under atmospheric pressure without post heat treatment. The doping concentration of Eu and Dy were fixed at 1% and 2% of the Ba + Mg component, respectively. The solutions were prepared by dissolving various amounts of the nitrate precursors of each component into a minimum amount of distilled water. The resulting solution was transferred into a china crucible, which was then introduced into a muffle furnace maintained at 500°C for 5-6 minutes. The voluminous and foamy combustion ash was easily milled to obtain the final $\text{Ba}_x\text{Mg}_y\text{Al}_2\text{O}_4:\text{Eu}^{2+}$ phosphor powders. XRD patterns of as-synthesized samples were recorded on an x-ray diffractometer with $\text{Cu K}\alpha = 1.5406 \text{ \AA}$, which was operated at 40 kV voltage and 40 mA anode current. Data were collected in 2θ values from 20° to 80° . The morphologies and sizes of the particles were examined using a PHI 700 Nano Scanning Auger Microprobe (Nano SAM) and a Shimadzu model ZU SSX – 550 Superscan scanning electron microscope (SEM), coupled with an energy dispersive x-ray spectrometer (EDS). Photoluminescence (PL) measurements were performed at room temperature on a Cary Eclipse fluorescence spectrophotometer (Model: LS 55) with a built-in 150 W xenon lamp as the excitation source and a grating to select a suitable wavelength for excitation.

3. Results and discussion

The present investigation aims at examining the relationship between the structural, morphological, photoluminescence properties and the compositions in the Eu^{2+} doped $\text{BaAl}_2\text{O}_4\text{-MgAl}_2\text{O}_4$ ternary and

quaternary systems. In our experiment, the Eu^{2+} doping concentration was fixed 1.5 % (molar ratio of Ba +Mg ions) for all the compositions, so that any changes in properties considered to be originating from the change in Ba/Mg molar ratios. Fig. 1(a) and (b) show representative pictures of the SEM micrographs of the $\text{Ba}_x\text{Mg}_y\text{Al}_2\text{O}_4:\text{Eu}^{2+}$ sample. It can be seen that the morphology of the synthesized powders is unconsolidated, reflecting the inherent nature of the combustion process (Fig. 1).

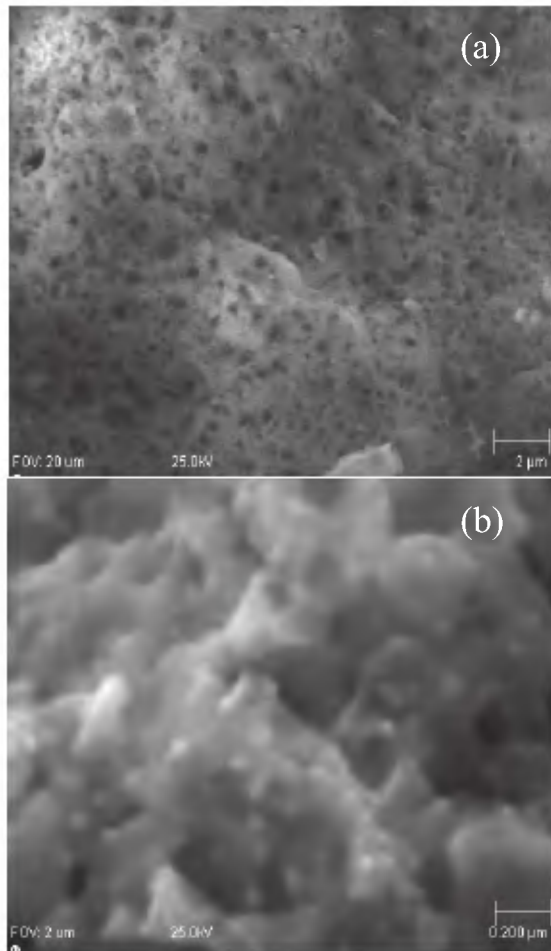


Figure 1 (a) and (b) are SEM image of $\text{Ba}_x\text{Mg}_y\text{Al}_2\text{O}_4:\text{Eu}^{2+}$.

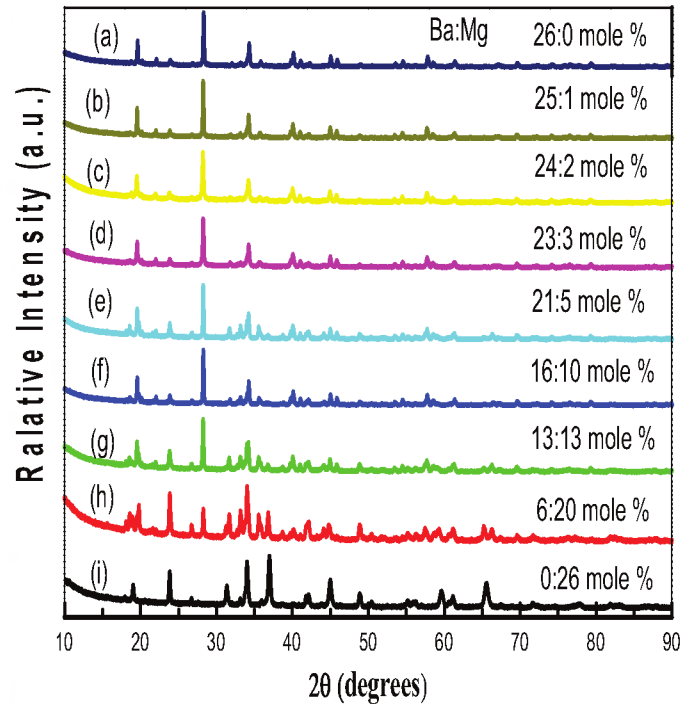


Figure 2 XRD patterns of $\text{Ba}_x\text{Mg}_y\text{Al}_2\text{O}_4:\text{Eu}^{2+}$ Ba:Mg mole% (a)26:0 , (b)25:1, (c)24:2 , (d) 23:3, (e) 21:4, (f) 16:10, (g) 13:13, (h) 6:20, and (i) 0:26.

The surfaces of the foams show a lot of cracks, voids and pores formed by the escaping gases during combustion reaction. In order to achieve accurate data of the grain size of $\text{Ba}_x\text{Mg}_y\text{Al}_2\text{O}_4:\text{Eu}^{2+}$ as-synthesized powders, its SEM image at high magnification recorded in Fig. 1(b). Most of the particles of $\text{Ba}_x\text{Mg}_y\text{Al}_2\text{O}_4:\text{Eu}^{2+}$ phosphor powders appear to be irregularly elliptical with aggregation and an average particle size of 30–50 nm (Fig. 1(b)). It is observed that the presence of Mg ions has minimum significance on the morphology of phosphors. A typical XRD patterns recorded for the $\text{Ba}_x\text{Mg}_y\text{Al}_2\text{O}_4:\text{Eu}^{2+}$ compositions with varying Ba/Mg concentrations were shown in Fig. 2. The examination of the diffraction patterns confirms that pure monoclinic phase BaAl_2O_4 (JCPDS: 82-2001) and pure orthorhombic MgAl_2O_4 (JCPDS:47-0254) are formed at Ba 26 mol% (Mg 0mol%) shown in Fig. 2(a) and Ba 0 mole%(Mg 26 mole%) displayed in Fig. 2(i), respectively. No other product or starting material was observed, implying that the phase composition of the synthesized powders are all low-temperature monoclinic phase for Ba 26mole % and orthorhombic for Mg 26mole% , and the little amount of doped rare earth ions have no noticeable change on the BaAl_2O_4 and MgAl_2O_4 phase composition [16]. Although no flux is added, $\text{Ba}_x\text{Mg}_y\text{Al}_2\text{O}_4:\text{Eu}^{2+}$ phase with high purity can be obtained at 500°C through the solution-combustion process to the starting materials, whereas it is

impossible to happen for solid-state reaction method due to impurities are formed at lower temperatures.

The excitation spectra of $\text{Ba}_x\text{Mg}_y\text{Al}_2\text{O}_4:\text{Eu}^{2+}$ powder phosphors are shown in Fig. 3(a) with strong excitation bands which could be attributed to a charge transfer band (CTB) of $\text{Eu}^{3+}-\text{O}$ band in the short ultraviolet region (240 nm) [22,23] for high Mg concentration and it can be seen clearly that the excitation spectra consist of a broad band with a maximum at about 340 nm, which can be attributed to the $\text{Ba}_x\text{Mg}_y\text{Al}_2\text{O}_4$ host excitation band for low Mg concentrations. The f-f transitions within the $\text{Eu}^{3+}, 4f^6$ configuration in longer wavelength region with ${}^7\text{F}_0 \rightarrow {}^5\text{D}_4$ (361 nm), ${}^7\text{F}_0 \rightarrow {}^5\text{L}_7$ (379 nm) and ${}^7\text{F}_0 \rightarrow {}^5\text{L}_6$ (393 nm) as the most prominent group. Fig. 3(b) shows the PL emission spectra of $\text{Ba}_x\text{Mg}_y\text{Al}_2\text{O}_4:\text{Eu}^{2+}$ powder phosphors excited at 240nm for low Mg concentration and 325 nm for high Mg concentration. The spectra tunes the emission colour from red to green as Ba:Mg concentration changes from 0:26 mole% to 26:0 mole%. The emission spectrum for Ba:Mg 0:26 mole% consists of strong and sharp peaks which are attributed to ${}^5\text{D}_0 \rightarrow {}^7\text{F}_J$ emission transitions, indicating the existence of Eu^{3+} ions in the $\text{MgAl}_2\text{O}_4:\text{Eu}^{2+}$ matrix. The spectra has emission peaks at 578, 592, 615, 656 and 690 nm which can be assigned to ${}^5\text{D}_0 \rightarrow {}^7\text{F}_J$ ($J=0, 1, 2, 3$ and 4) [24,25] transitions of Eu^{3+} ions namely the ${}^5\text{D}_0 \rightarrow {}^7\text{F}_0$ (578 nm), ${}^5\text{D}_0 \rightarrow {}^7\text{F}_1$ (592 nm), ${}^5\text{D}_0 \rightarrow {}^7\text{F}_2$ (615 nm), ${}^5\text{D}_0 \rightarrow {}^7\text{F}_3$ (656 nm), and ${}^5\text{D}_0 \rightarrow {}^7\text{F}_4$ (694 nm), respectively. Since 4f electrons are shielded by 5s and 5p electrons in the outermost shells of the europium ion, as a result narrow emission peaks are expected, consistent with the sharp and intense peak around 615 nm and is due to the ${}^5\text{D}_0 \rightarrow {}^7\text{F}_2$ transition, based on selection rules [26,27]. The intensity for ${}^5\text{D}_0 \rightarrow {}^7\text{F}_2$ red (615 nm) emission is much stronger than that of the orange 592nm emission.

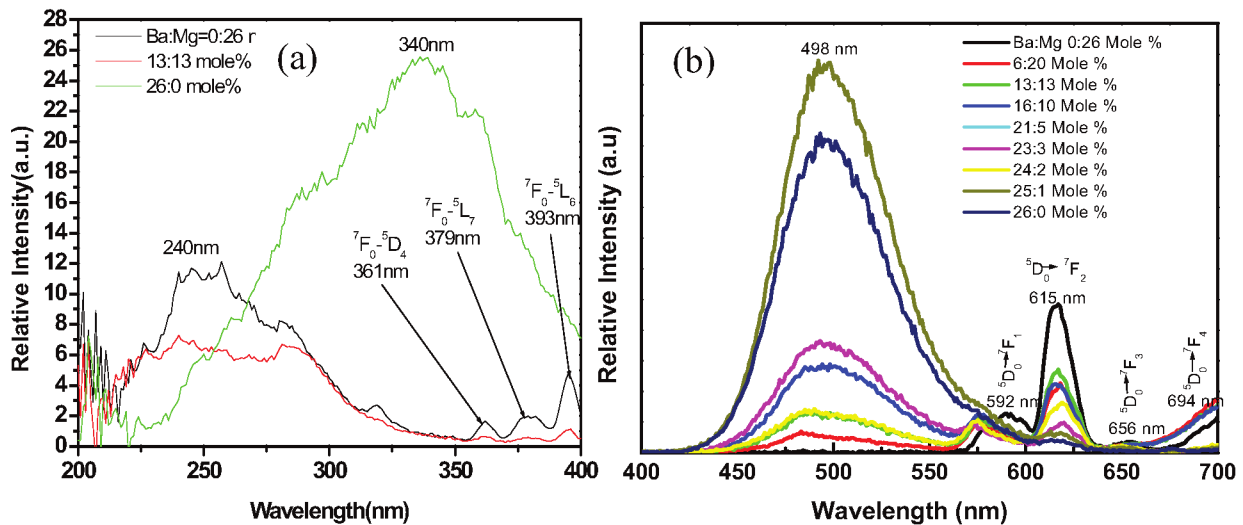


Figure 3 (a) Excitation spectra, and (b) Emission spectra of $\text{Ba}_x\text{Mg}_y\text{Al}_2\text{O}_4:\text{Eu}^{2+}$ powder phosphors.

On the other hand, the symmetrical band blue-green emission at 498 nm for Ba:Mg 26:0 mole% is attributed to the typical transition between the ground state ($4f^7$) and the excited state ($4f^6 5d^1$) of Eu^{2+} ions [28]. They compare very well with the results of Lu et al. [29].

The Luminescent decay curve of $\text{Ba}_x\text{Mg}_y\text{Al}_2\text{O}_4:\text{Eu},\text{Dy}$ phosphor monitored at 615 nm for different Ba:Mg mole ratio was shown in Fig. 4. The decay behaviour analysed using curve fitting [30], relying on the following triple exponential equation:

$$I = I_1 \exp\left(-\frac{t}{\tau_1}\right) + I_2 \exp\left(-\frac{t}{\tau_2}\right) + I_3 \exp\left(-\frac{t}{\tau_3}\right) \quad (1)$$

where I represents the phosphorescent intensity; I_1 , I_2 and I_3 are constants; t is the time; τ_1 , τ_2 and τ_3 are the decay constants, deciding the decay rate for the fast, medium and slow exponentially decay components, respectively.

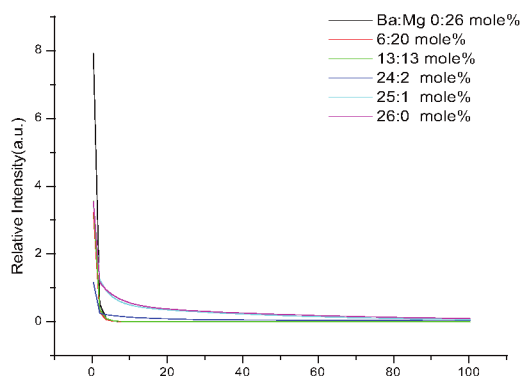


Figure 4 Afterglow characteristics of $\text{Ba}_x\text{Mg}_y\text{Al}_2\text{O}_4:\text{Eu,Dy}$ powder

Ba:Mg mole ratio	0:26	6:20	13:13	24:2	25:1	26:0
Component	Decay Constants (s)					
Fast (τ_1)	1.20	0.57	1.73	0.39	0.21	0.31
Medium (τ_1)	0.35	0.22	0.63	9.14	3.33	59.58
Slow (τ_1)	0.55	1.48	0.21	127.86	47.41	4.97

Table 1 Results for fitted decay curves of the phosphor powders with different Mg:Ba molar ratios

The fitting results of parameters of τ_1 , τ_2 and τ_3 are listed in Table 1. Three components namely slow, medium, and fast component are responsible for the persistent luminescence from the synthesized phosphor.

4. Conclusion

In conclusion, excellent tuning green-red $\text{Ba}_x\text{Mg}_y\text{Al}_2\text{O}_4:\text{Eu}^{2+}$ nanophosphors were successfully synthesized at low temperature 500°C using the solution - combustion with optimized condition Eu^{2+} doping concentration fixed as 1.5 % (molar ratio of Ba +Mg ions). XRD data was analyzed for the phase stability and crystallinity and observed that pure monoclinic phase diffraction peaks of BaAl_2O_4 are predominant for low Mg concentration and orthorhombic MgAl_2O_4 for low Ba mole concentration. The synthesized $\text{Ba}_x\text{Mg}_y\text{Al}_2\text{O}_4$ phosphor doped with Eu^{2+} ions can be efficiently excited by 325nm UV radiation for low Ba concentration and by 240nm shorter UV for low Mg concentration and gives dominant emission band peaking at 615nm(red) and 498nm(green), respectively. The nature and structural details of this phosphor have been investigated from the measurement of XRD and SEM. Based on the emission analysis results; we suggest that it is a novel tuning green-red colors emitting optical material with potential luminescent applications.

References

- [1] L. Zhou, W.C.H. Choy, J. Shi, M. Gong and H. Liang 2006 Mater. Chem. Phys. **100** 372
- [2] B. Yan and X.Q. Su 2007 Opt. Mater. **29** 547
- [3] W.B. Im, Y.I. Kim, J.H. Kang and D.Y. Jeon 2005 Solid State Commun. **134** 717
- [4] Y.Q. Li, C.M. Fang, G. de With and H.T. Hintzen 2004 J. Solid State Chem. **177** 4681
- [5] M. Yu, J. Lin, J. Fu, H.J. Zhang and Y.C. Han 2003 J. Mater. Chem. **13** 1413.
- [6] M. Leskel and L. Niinistö 1992 Mater. Chem. Phys. **31** 7
- [7] G. Blasse, B.C. Grabmaier, Luminescent Materials, Springer, Berlin, 1994.
- [8] T. Matsuzawa, Y. Aoki, M. Takeuchi and Y. Murayama "A New Long- Phosphorescent Phosphor with High Brightness, $\text{SrAl}_2\text{O}_4:\text{Eu}^{2+},\text{Dy}^{3+}$ "; p. 160 in *Proceedings of 188th Meeting of the Electrochemical Society* (Chicago, IL, Oct. 8–13, 1995).
- [9] Y. Murayama 1996 Sci. Am. Jpn., **26** 20
- [10] Y. Lin, Z. Zhang, F. Zhang, Z. Tang and Q. Chen 2000 Mater. Chem. Phys. **65** 103

- [11] W. Jia, H. Yuan, L. Lu, H. Liu and W.M. Yen 1998 *J. Lumin.* **76–77** 424
- [12] X.Q. Piao, K.-I. Machida, T. Horikawa, H. Hanzawa, Y. Shimomura and N. Kijima 2007 *Chem. Mater.* **19** 4592
- [13] Y.Q. Li, A.C.A. Delsing, G.D. With and H.T. Hintzen 2005 *Chem. Mater.* **17** 3242
- [14] F.C. Palilla, A.K. Levine and M.R. Tomkus 1968 *J. Electrochem. Soc.* **115** 642
- [15] R.P. Rao 1996 *J. Electrochem. Soc.* **143** 189
- [16] Y. Lin, Z. Zhang, F. Zhang, Z. Tang and Q. Chen 2000 *Mater. Chem. Phys.* **65** 103
- [17] L.K. Kurihara and S.L. Suib 1993 *Chem. Mater.* **5** 609
- [18] J.J. Kingsley, K. Suresh and K.C. Patil 1990 *J. Mater. Sci.* **25** 1305
- [19] S.T. Aruna and A. S. Mukasyan 2008 *Curr. Opin. Solid ST. M.* **12** 44
- [20] K. C. Patil, S. T. Aruna and T. Mimani 2002 *Curr. Opin. Solid ST. M.* **6** 507
- [21] R. Ianos and I. Lazau 2009 *Mater. Chem. Phys.* **115** 645
- [22] M. Yu, J. Lin, Y.H. Zhou, S.B.Wang, 2002 *Mater. Lett.* **56** 1007
- [23] G. Blasse 1966 *J. Chem. Phys.* **45** 2356
- [24] H. You, M. Nogami 2005 *J. Phys. Chem. B* **109** 13980
- [25] B. Vengala Rao, U. Rambabu and S. Buddhudu 2006 *Physica B* **382** 86
- [26] B.R. Judd 1962 *Phys. Rev.* **127** 750
- [27] G.S. Ofelt 1962 *J. Chem. Phys.* **37** 511
- [28] G. Blasse and B.C. Grabmaier, “Luminescent Materials” (Springer-Verlag, Berlin, 1994) p.33.
- [29] Y.Q. Lu, Y.X. Li, Y.H. Xiong, D. Wang and Q.R. Yin 2004 *Microelectron. J.* **35** 379
- [30] Sakai R, Katsumata T, Komuro S and Morikawa T 1999 *J. Lumin.* **85** 149